European Journal of Chemistry 6 (3) (2015) 314-318

European Journal of Chemistry

Journal webpage: www.eurjchem.com

Synthesis, characterization and ionic conductivity of $MgAl_2O_4$

Abdelhakim Elmhamdi and Kais Nahdi *

Laboratoire d'Application de la Chimie aux Ressources et Substances Naturelles et à l'Environnement (LACReSNE), Faculté des Sciences de Bizerte, Université de Carthage, 7021 Bizerte, Tunisie

** Corresponding author at: Laboratoire d'Application de la Chimie aux Ressources et Substances Naturelles et à l'Environnement (LACReSNE), Faculté des Sciences de Bizerte, Université de Carthage, 7021 Bizerte, Tunisie.*
Tel.: +216.72.590717. Fax: +216.72.590566. E-mail address: k_nahdi@yahoo.fr (K. Nahdi).

ARTICLE INFORMATION

DOI: 10.5155/eurjchem.6.3.314-318.1276

Received: 01 June 2015
Accepted: 28 June 2015
Published online: 30 September 2015
Printed: 30 September 2015

KEYWORDS

$MgAl_2O_4$
Jonscher law
Citrate sol-gel
Ac conductivity
Activation energy
Impedance spectroscopy

ABSTRACT

Magnesium aluminate nanoparticles have been synthesized by a citrate sol-gel route. X-ray diffraction and IR spectroscopy study confirmed the formation of $MgAl_2O_4$ cubic spinel structure without presence of any secondary phase. Crystallite size of the synthesized nanoparticles was found to be equal to 24 nm. The ac conductivity of $MgAl_2O_4$ was studied using complex impedance spectroscopy technique in the frequency range from 5 Hz to 13 MHz and temperature range from 673 to 798 K. The temperature and frequency dependence of ac conductivity were highlighted and the activation energies of, respectively, ac conduction and relaxation processes were also calculated.

Cite this: *Eur. J. Chem.* **2015**, *6(3)*, 314-318

1. Introduction

The spinel phase is a mixed oxide with general formula of AB_2O_4. It is an association between one divalent cation (A^{2+}), and two trivalent cations (B^{3+}). The unit cell consists of a face-centered cubic arrangement of oxygen ions containing 32 O ions, 64 tetrahedral and 32 octahedral sites which are occupied with A^{2+} and B^{3+} cations [1,2]. When one half of the octahedral interstices are occupied by the B^{3+} cations and one-eighth of the tetrahedral sites are occupied by the A^{2+} cations the spinel phase is called "normal". Whereas, when tetrahedral sites are occupied by half of the B^{3+} and octahedral sites are occupied by the other half and A^{2+} the spinel phase is called "inverse".

Spinel phase with chemical formula $MgAl_2O_4$ is the mineral type of this oxide family. Thanks to its high thermal stability (melting point at 2135 °C), high hardness (16 GPa), high mechanical resistance, high resistance against chemical attack, wide band gap energy, high electrical resistivity, relatively low thermal expansion coefficient (9.10^{-6} 1/°C) between 30 and 1400 °C, low dielectric constant (ε = 7.5), low density 3.58 g/cm^3, high thermal shock resistance, hydrophobicity and low surface acidity, $MgAl_2O_4$ has been widely used in various applications such as in metallurgical, electrochemical, radiotechnical and chemical industrial fields [3-10].

Several studies have focused on the preparation of $MgAl_2O_4$ phase using different methods such as, conventional solid-state-reaction, sol-gel, spray drying (atomization), co-precipitation, microwave, hydroxide co-precipitation, hydro-thermal, modified pechinic process, and organic gel-assisted citrate complexation [5,6,11-42]. The preparation method affects not only the purity and the reactivity of the obtained $MgAl_2O_4$ but also the physical properties such as the electrical conductivity. Few works have focused on the investigation of the electrical properties of $MgAl_2O_4$ [43-47]. The first work [43] have studied the electrical properties of both thin film and bulk $MgAl_2O_4$ at 313 K and in environments at different relative humidity values between 2 and 95%, using ac impedance spectroscopy in 0.1 Hz - 10 kHz frequency range. The second work [44] deals with the study of conductivity and dielectric properties of magnesium aluminate nanoparticles in the temperature range 303-450 K and frequency range 200 Hz - 4 MHz. Recently the dielectric properties [45-47], DC conductivity [45] and AC conductivity [47] of $MgAl_2O_4$ were investigated. The experimental conditions and the principal results of the above mentioned works are summarized in Table 1.

Our work is a contribution to the investigation of the electrical properties of $MgAl_2O_4$ carried out in a larger frequency range from 5 Hz to 13 MHz and in higher temperature range from 673 to 798 K.

ISSN 2153-2249 (Print) / ISSN 2153-2257 (Online)
http://dx.doi.org/10.5155/eurjchem.6.3.314-318.1276

Table 1. Literature data for electrical conductivity study of $MgAl_2O_4$.

Frequency	Temperature (K)	E_a (eV)	Reference
0.1 Hz - 10 kHz	313	-	[43]
200 Hz - 4 MHz	303-450	-	[44]
1 khz - 1 MHz	293-673	0.770	[45]
200 Hz - 100 kHz	Room temperature	-	[46]
0.01 Hz - 10 MHz	423-573	E1 = 0.1828 (T < 503 K), E2 = 0.8791 (T > 503 K)	[47]

The AC conductivity was calculated. The temperature and frequency dependence of ac conductivity were highlighted and the activation energies of, respectively, ac conduction and relaxation processes were also calculated.

2. Experimental

2.1. Instrumentations

X-ray diffraction (XRD) patterns have been recorded with a Bruker D8-Advance diffractometer using CuKα radiation (λ = 1.5406 Å). XRD data have been collected over the 15-70 ° 2θ range, at the scan speed of 1.2 °/min and 0.02 ° step. The crystalline phases have been identified using the International Centre for Diffraction Data (ICDD) powder diffraction files. Fourier transformed infrared (FT-IR) spectrum has been obtained with a Bruker spectrometer, in the 4000-400 cm^{-1} range, using the KBr pellet technique. Electrochemical Impedance Spectra (EIS) were obtained using a Hewlett-Packard HP 4192 analyser. The impedance measurements were taken in an open circuit using two electrode configurations with signal amplitude of 50 mV and a frequency band ranging from 5 Hz to 13 MHz. Powder have been pressed under 5 tons/cm^2 and sintered at 1523K to prepare the pellet. Both pellet surfaces were coated with silver pastes electrodes while the platinum wires attached to the electrodes were used as current collectors. Electrodes have been then heated at 1028 K to ensure good electrical contacts. All these measurements were performed at equilibrium potential at high temperature ranging between 673 and 798 K in air atmosphere. In order to obtain the bulk, grain boundary and total ionic conductivities, the resulting data was analysed using the equivalent circuit of the Zview software [48].

Conductivity values have been estimated with help of the following relation:

$$\sigma = \frac{l}{RS} \quad (1)$$

where R is the resistance deduced from impedance diagrams and S and l are the area and the thickness of pellets, respectively.

The temperature dependence of conductivity was calculated using the following Arrhenius Equation (2),

$$\sigma T = A \times exp\left(\frac{-E_a}{KT}\right) \quad (2)$$

where A is the pre-exponential factor (which is related to the effective number of mobile species), E_a the activation energy of the conduction process, K Boltzmann's constant and T the absolute temperature.

2.2. Synthesis

Magnesium chloride ($MgCl_2.6H_2O$), aluminum chloride ($AlCl_3$) and citric acid ($(HOCO-CH_2)_2C(OH)-COOH$) were used as starting chemicals for the preparation of $MgAl_2O_4$spinel phase particles by citric assisted gel-combustion method. Magnesium and aluminum chlorides were dissolved, in appropriate molar ratio, in distilled water then an excess of citric acid, initially dissolved in water, was added. The mixture was kept under stirring at 80 °C until complete evaporation of the liquid phase. The resulting gel was dried overnight at 100 °C then calcined at 900 °C for 4 h.

3. Results and discussion

3.1. X-ray diffraction studies

Figure 1 is represented the powder X-ray diffraction pattern of the prepared $MgAl_2O_4$ obtained after heat treatment of the citric precursor at 900 °C. The observed diffraction peaks centered at 4.66, 2.84, 2.42, 2.01, 1.65, 1.55, 1.43 and 1.36 Å corresponds to the standard JCPDS Card No77-0435 data of a pure crystalline phase of $MgAl_2O_4$ spinel structure. The calculated lattice parameter of $MgAl_2O_4$ is found to be 8.0831 Å which is close to the reported value of the magnesium aluminate. The space group Fd-3m is so confirmed. The average crystallite size of the prepared annealed sample was determined from X-ray line broadening using the Scherrer formula and it is found to be 24 nm.

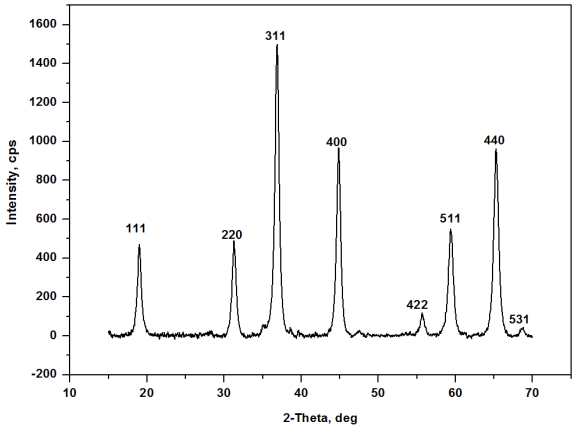

Figure 1. X-ray diffraction pattern of prepared $MgAl_2O_4$.

The observed diffraction peaks at 4.66, 2.84, 2.42, 2.01, 1.65, 1.55, 1.43 and 1.36 Å are attributed to the lattice plane (111), (220), (311), (400), (422), (511), (440) and (531), respectively, and these are well matched with the reported values [40,41,49].

3.2. Infrared spectroscopy (FT-IR)

Figure 2 is represented the IR spectrum of the prepared $MgAl_2O_4$ obtained after heat treatment of the citric precursor at 900 °C. It exhibits two absorption bands centered at 512 and 685 cm^{-1}. These bands are attributed to the stretching vibration of Mg-O in MgO_4 tetrahedral and of Al-O in AlO_6 octahedral groups, respectively, in the $MgAl_2O_4$ spinel structure [40-42].

3.3. Electrical conductivity

3.3.1. Complex electrical impedance analysis

Typical complex impedance spectra (Nyquist plots: -Z'' *vs* Z') of $MgAl_2O_4$, in the frequency range from 13 MHz to 5 Hz

and temperature range from 673 to 798 K, are shown in Figure 3.

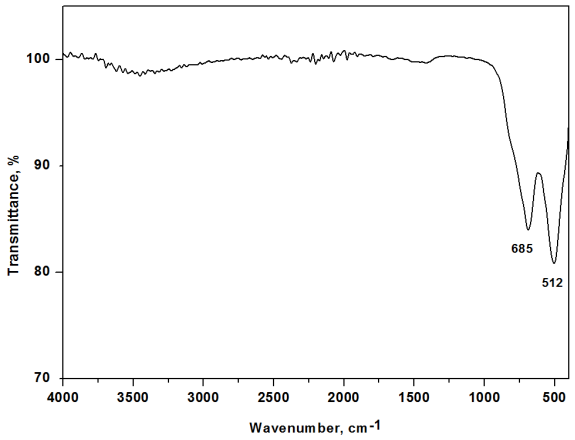

Figure 2. FT-IR spectrum of prepared $MgAl_2O_4$.

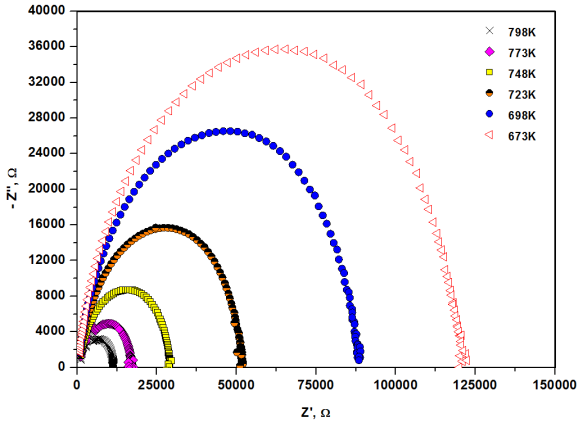

Figure 3. Nyquist plots of $MgAl_2O_4$ at different temperature.

The impedance spectra of the pellet prepared sample, at different temperature, are characterized by a complete single semicircular arc. The absence of a second semicircle at higher frequency in complex impedance plots suggests the dominance of bulk over the grain boundary contribution in the studied frequency range.

The decreases of curvature radius when temperature increases, observed in Figure 3, can be attributed to the presence of single electrical relaxation phenomena in the material under investigation [50], the bulk resistance of $MgAl_2O_4$ decreases and hence the electrical conductivity increases.

The analysis results of the impedance spectra are shown in Table 2. Here, the bulk resistance was calculated from the intercept of the semicircle with the real axis and the total conductivity of $MgAl_2O_4$ pellet was calculated using Equation (1). The conductivity of the studied sample reaches the value of 8.44970×10^{-6} S/cm at 798 K.

Table 2. Resistance and conductivity of $MgAl_2O_4$ at different temperatures.

Temperature (K)	Resistance (Ω)	Conductivity ($\sigma.10^{-6}$, $S.cm^{-1}$)
673	1.2486×10^5	0.0755865
698	93118	1.01301
723	52443	1.80005
748	29118	3.24198
773	17046	5.53796
798	11172	8.44970

3.3.2. AC Conductivity

AC conductivity measurement is an important tool for studying the ionic transport properties of materials. When an ac electric current passes through the solid electrolyte, processes like ion motion through bulk of the electrolyte, charge transfer across the electrode-electrolyte interface, *etc.*, take place.

3.3.2.1. Temperature dependence of AC conductivity

Figure 4 shows the Arrhenius plot of Ln(σT) *vs* 1000/T. The activation energy calculated from the slope of the Arrhenius plot was found equal to 1.11 eV. The goodness of the fit (r = 0.9992) all along the studied temperature range indicates the existence of a unique conduction mechanism due to the transfer of electrons between Al^{3+} and Mg^{2+} ions through hopping conduction mechanism.

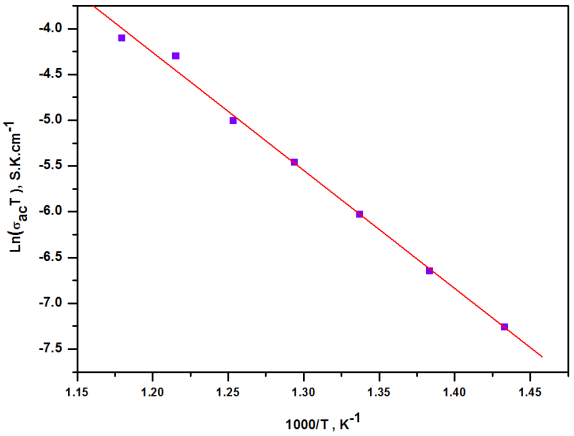

Figure 4. Arrhenius plot of the electronic conductivity of $MgAl_2O_4$.

3.3.2.2. Frequency dependence of AC conductivity

Figure 5 illustrates the frequency (ω) dependence of ac conductivity (σ_{ac}) at different temperatures of $MgAl_2O_4$ sample. The corresponding curves exhibit two distinctly frequency regions which can be separated by a change in the slope for each temperature.

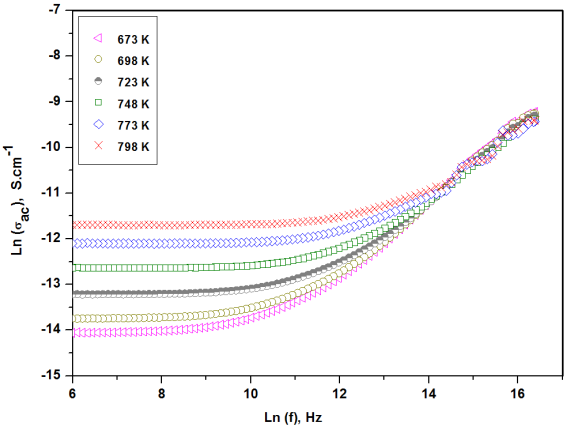

Figure 5. Frequency dependence of AC conductivity at different temperatures.

The frequency at which the slope of ac conductivity changes is known as the "hopping frequency, ω_p". It is

important to note that the values of hopping frequencies are observed to go up with the increase in temperature. Figure 5 shows that σ_{ac} increases with increasing frequency and becomes independent of frequency after a certain value. At higher frequencies, the values of ac electrical conductivity become closer, and are temperature-independent. The frequency dependence of conductivity displays two different regimes that can be described using the Jonscher's universal power law [51]:

$$\sigma_{ac}(\omega) = \sigma(0) + A\omega^{s} \quad (3)$$

where σ(0) is the dc conductivity obtained from the extrapolation to zero frequency of $\sigma_{ac}(\omega)$, A is a constant and s is the frequency exponent describing ion-ion interactions in hopping process; i.e., the exponent n would be 0 for random ion hopping (absence of interactions) whereas it tends to1 for fully correlated ion motions [52,53].

Figure 6 shows the dependence of the imaginary part of impedance (-Z'') of $MgAl_2O_4$ on frequency at different temperatures. Each curve shows a maximum that shifts to higher frequencies when temperature increases.

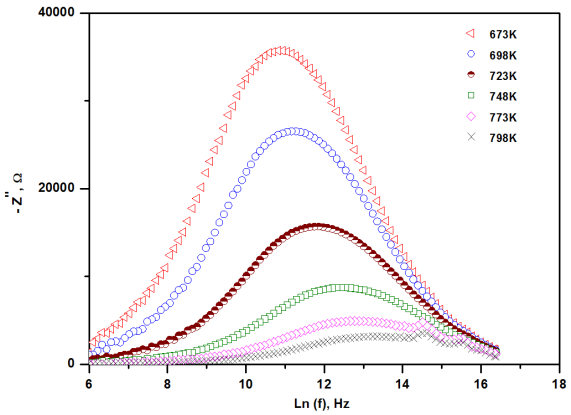

Figure 6. Frequency dependence of the imaginary part (-Z'').

The appearance of this maximum at a particular frequency (f_{max}) is an indication of a thermally activated electrical relaxation process in the material when temperature increases. The broadening of peaks on increasing temperature confirms the existence of temperature dependent relaxation phenomena in $MgAl_2O_4$.

The impedance data are used to evaluate the relaxation time (τ) of the electrical phenomena in $MgAl_2O_4$ using the following relation:

$$\tau = \frac{1}{2\pi f_{max}} = RC \quad (4)$$

where f_{max} is the relaxation frequency. The variation of τ with temperature is shown in Figure 7. This plot shows a steady increase in the relaxation time with rising temperature. This result suggests the presence of temperature-dependent electrical relaxation phenomena in the material, possibly due to the migration of species/defects. The curve was found to follow the Arrhenius relation:

$$\tau = \tau_0 exp\left(\frac{E_{a\tau}}{KT}\right) \quad (5)$$

where τ_0 is a pre-exponential factor, $E_{a\tau}$ is the activation energy of the relaxation phenomena, K is the Boltzmann constant and T is the absolute temperature. Activation energies ($E_{a\tau}$) estimated from the slope of the ln(τ) against 1000/T curve is found equal to 0.98 eV.

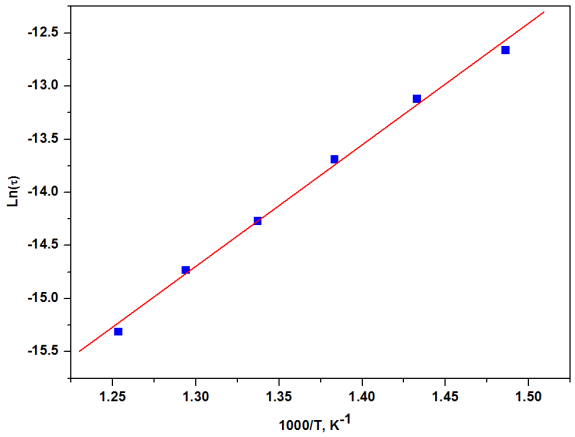

Figure 7. Dependence of the relaxation time with inverse of temperature in $MgAl_2O_4$.

4. Conclusion

$MgAl_2O_4$ of high purity and 24 nm grain size has been prepared by citric assisted gel-combustion method. The characterization of the obtained powder at 900 °C by XRD and FT-IR techniques confirms the obtaining of a pure nano-crystalline of $MgAl_2O_4$ with spinel structure. The electrical properties of $MgAl_2O_4$ were studied using complex impedance spectroscopy. The analysis of the impedance data showed that (i) The calculated conductivity value of nanocrystalline $MgAl_2O_4$ pellet at 798 K is found to be 8.4497×10^{-6} S/cm. (ii) The corresponding activation energy follows the Arrhenius law, which was found equal to 1.11 eV. (iii) The relaxation frequencies shift to a higher frequency side with increasing temperature. (iv) The activation energy of the relaxation process is equal to 0.98 eV and (v) The frequency dependence of ac conductivity data follows the 'universal' power Jonscher's law in $MgAl_2O_4$.

Acknowledgements

The authors thank Dr. Abdelwahab Inoubli and Dr. Massoud Kahlaoui (Laboratoire de Physique des Matériaux, Faculté des Sciences de Bizerte-Université de Carthage) for the conductivity measurements. The authors would also like to thank the language expert Samar Amri Epouse Dridi for proofreading the manuscript.

References

[1]. Sickafus, K. E.; Wills, J. M. *J. Am. Ceram. Soc.* **1999**, *82(12)*, 3279-3292.
[2]. Wyckoff, R. W. G. Wiley Interscience, New York, 1964.
[3]. Yamakawa, A.; Hashiba, M.; Nurishi, Y. *J. Mater. Sci.* **1989**, *24*, 1491-1498.
[4]. Ganesh, I.; Srinivas, B.; Johnson, R.; Saha, B. P.; Mahajan, Y. R. *Br. Ceram. Trans.* **2002**, *101*, 247-254.
[5]. Ganesh, I.; Johnson, R.; Rao, G. V. N.; Mahajan, Y. R.; Madavendra, S. S.; Reddy, B. M. *Ceram. Int.* **2005**, *31*, 67-74.
[6]. Adak, A. K.; Saha, S. K.; Pramanik, P. *J. Mater. Sci. Lett.* **1997**, *16*, 234-235.
[7]. Ganesh, I.; Bhattacharjee, S.; Saha, B. P.; Johnson, R.; Rajeshwari, K.; Sengupta, R.; Ramanarao, M. V.; Mahajan, Y. R. *Ceram. Int.* **2002**, *28(3)*, 245-253.
[8]. Bhaduri, S.; Bhaduri, S. B. *Ceram. Int.* **2002**, *28(2)*, 153-158.
[9]. Ji-Guang Lee, T. I.; Lee, J. H.; Mori, T. *J. Am. Ceram. Soc.* **2000**, *83(11)*, 2866-2868.
[10]. Baudin, C.; Martinez, R.; Pena, P. *J. Am. Ceram. Soc.* **1995**, *78*, 1857-1862.
[11]. Ryshekewitch, E. Oxide Ceramics, Academic Press, New York 1960, pp. 257.
[12]. Kriegel, W. W.; Palmer III, H.; Choi, D. M. *Spec. Ceram.* **1964**, *3*, 167-186.
[13]. Bakker, W. T.; Lindsay, L. G. *Am. Ceram. Soc. Bull.* **1967**, *46*, 1094-1097.

[14]. Bailey, J. T.; Russell, R. *Am. Ceram. Soc. Bull.* **1968**, *47*, 1025-1029.
[15]. Hamono, K.; Kanzaki, S. J. *Ceram. Soc. Jpn*. **1977**, *85*, 225-230.
[16]. Kostic, E.; Momcilovic, L. *Ceramurgia Int.* **1977**, *3*, 57-60.
[17]. Teoreanu, I.; Ciocea, N. *Interceram*. **1987**, *4*, 19-21.
[18]. Park, H. C.; Lee, Y. B.; Oh, K. D.; Riley, F. L. *J. Mater. Sci. Lett.* **1997**, *16*, 1841-1844.
[19]. Sarkar, R.; Das, S. K.; Banerjee, G. *Ceram. Int.* **1999**, *25*, 485-489.
[20]. Sarkar, R.; Banerjee, G. J. *Eur. Ceram. Soc*. **1999**, *19*, 2893-2900.
[21]. Zografou, C.; Reynen, P.; Van Mallinckrodt, D. *Interceram*. **1983**, *38*, 37-39.
[22]. Zografou, C.; Reynen, P.; Van Mallinckrodt, D. *Interceram*. **1983**, *38*, 40-43.
[23]. Serry, M. A.; Hammad, S. M.; Zawrah, M. F. *Br. Ceram. Trans.* **1998**, *97*, 275-282.
[24]. Domanski, D.; Urretavizcaya, G.; Castro, F. J.; Gennan, F. C. *J. Am. Ceram. Soc.* **2004**, *87*, 2020-2024.
[25]. Angappan, S.; Berchmans, L. J.; Augustin, C. O. *Mater. Lett.* **2004**, *58*, 2283-2289.
[26]. Chen, S. K.; Cheng, M. Y.; Lin, S. J. *J. Am. Ceram. Soc.* **2002**, *85*, 540-544.
[27]. Ghosh, A.; Das, S. K.; Biswas, J. R.; Tripathi, H. S.; Banerjee, G. *Ceram. Int*. **2000**, *26*, 605-608.
[28]. Ganes, I.; Bhattacharjee, S.; Saha, B. P.; Johnson, R.; Mahajan, Y. R. *Ceram. Int.* **2001**, *27*, 773-779.
[29]. Li, J. G.; Ikegami, T.; Lee, J. H.; Mori, T. *J. Am. Ceram. Soc.* **2000**, *83*, 2866-2868.
[30]. Yang, N.; Chang, L. *Mater. Lett.* **1992**, *15*, 84-88.
[31]. Behera, S. K.; Barpanda, P.; Pratihar, S. K.; Bhattacharyya, S. *Mater. Lett.* **2004**, *58*, 1451-1455.
[32]. Zhang, H.; Jia, X.; Liu, Z.; Li, Z. *Mater. Lett.* **2004**, *58*, 1625-1628.
[33]. Debsikdar, J. C. *J. Mater. Sci.* **1985**, *20*, 4454-4458.
[34]. Naskar, M. K.; Chatterjee, M. *J. Am. Ceram. Soc.* **2005**, *88*, 38-44.
[35]. Guo, J.; Lou, H.; Zhao, H.; Wang, X.; Zheng, X. *Mater. Lett.* **2004**, *58*, 1920-1923.
[36]. Bratton, R. J. *Ceram. Bull.* **1969**, *48(8)*, 759-762.
[37]. Ayman, A. A.; Mahmud, R. A.; Teymur, M. I. *Casp. J. Appl. Sci. Res*. **2013**, *2(2)*, 85-90.
[38]. Kakooei, S.; Rouchi, J.; Mohammad, E.; Alimanesh, M.; Dehzangi, A. *Casp. J. Appl. Sci. Res.* **2012**, *1(13)*, 16-22.
[39]. Pacurariu, C.; Lazau, I.; Ecsedi, Z.; Lazau, R.; Barvinschi, P.; Marginean, G. J. *Eur. Ceram. Soc.* **2007**, *27*, 707-710.
[40]. Saberi, A.; Golestani-Fard, F.; Sarpoolaky, H.; Willert-Porada, M.; Gerdes, T.; Simon, R. J. *Alloy. Compd.* **2008**, *462*, 142-146.
[41]. Marakkar, P. V. K.; Subrata, D. *Ceram. Int.* **2013**, *39*, 7891-7894.
[42]. Alvar, E. N.; Rezaei, M.; Alvar, H. N. *Powder Technol.* **2010**, *198*, 275-278.
[43]. Gualtiero, G.; Giampiero, M.; Enrico, T. *J. Am. Ceram. Soc.* **1993**, *76*, 743-750
[44]. Kurien, S.; Sebastian, S.; Mathew, J.; George, K. C. *Indian J. Pure Appl. Phys.* **2004**, *42*, 926-933.
[45]. Iqbal, M. J.; Ismail, B. J. *J. Alloys Compd.* **2009**, *472*, 434-440.
[46]. Saha, S.; Das, B.; Mazumder, N.; Bharati, A.; Chattopadhyay, K. K. J. *Sol-Gel Sci. Technol.* **2012**, *61*, 518-526.
[47]. Padmaraj, O.; Venkateswarlu, M.; Satyanarayana, N. *Ceram. Int.* **2015**, *41*, 3178-3185.
[48]. Massoud, K.; Sami, C.; Abdelwahab, I.; Adel, M.; Chaabane, C. *Ceram. Inter.* **2013**, *39*, 3873–3879
[49]. Pacurariu, C.; Lazau, I.; Ecsedi, Z.; Lazau, R.; Barvinschi, P.; Marginean, G. J. *Eur. Ceram. Soc.* **2007**, *27*, 707-710.
[50]. Molak, A.; Paluch, M.; Pawlus, S.; Klimontko, J.; Ujma, Z.; Gruszka, I. *J. Phys. D Appl. Phys.* **2005**, *38*, 1450-1460.
[51]. Jonscher, A. K. *Nature* **1977**, *267*, 673-679.
[52]. Funke, K. *J. Non-Cryst. Solids* **1994**, *1215*, 172-174.
[53]. Ngai, K. L.; Tsang, K. Y. *Phys. Rev. E* **1999**, *60*, 4511-4517.